

*Original Research*

# Research on Remote Sensing Identification Model of Urban Malodorous Black Water in Pearl River Estuary Based on High-resolution Image

Lei Su<sup>1</sup>, Yan Zhou<sup>2,3</sup>, Lei Fan<sup>2,3\*</sup>, Junying Li<sup>4</sup>, Yang Huang<sup>5</sup>

<sup>1</sup>Zhongshan Institute, University of Electronic Science and Technology, Zhongshan 528402, China

<sup>2</sup>Forestry College, Shenyang Agricultural University, Shenyang 110161, China

<sup>3</sup>Key Laboratory of Northern Landscape Plants and Regional Landscape (Liaoning Province), Shenyang 110161, China

<sup>4</sup>Architectural and Civil Engineering College, Huizhou University, Huizhou 516007, China

<sup>5</sup>Institute of Architectural Engineering, Beibu Gulf University, Qinzhou 535011, China

*Received: 25 September 2022*

*Accepted: 12 October 2022*

## Abstract

Taking some water areas in Zhongshan as the research object, 62 sampling points are selected to analyze the spectral characteristics of malodorous black waters and normal waters. According to this characteristic, this study tries to strengthen the differences between malodorous black waters and normal waters by using a new band combination method, and establishes discrimination models HCI on malodorous black waters, which are compared with the traditional NDBWI and BOI index models. Results show that: (1) The recognition accuracy of ratio algorithm is significantly higher than that of difference algorithm. (2) Selecting different water quality samples to draw the box diagram of each index model as an important basis for defining the threshold, the NDBWI threshold is 0.09, the BOI threshold is 0.06 and the HCI5 threshold is 0.4. (3) Using the synchronous monitoring results of surface water quality to evaluate the identification accuracy of malodorous black waters, the Kappa coefficient is the highest in HCI5 (0.876) and BOI (0.843), followed by NDBWI (0.739) and HCI4 (0.608). (4) The BOI and HCI5 index models are applied to other remote sensing images of Zhongshan City, and they can still distinguish malodorous black waters from normal waters, and have certain universality. Accordingly, this study suggests that BOI and HCI5 should be used as index models for remote sensing identification of malodorous black waters in this area.

**Keywords:** high score image, multi-spectrum, malodorous black waters, remote sensing identification, city of Pearl river estuary

## Introduction

Malodorous black waters refer to the waters with unpleasant color and/or unpleasant odor in the urban built-up area [1]. The „black odor“ phenomenon is mainly caused by the emission of external pollutants, the release of internal pollution, the high gradient change of water temperature and the lack of hydrodynamic conditions [2, 3], which has become a common environmental pollution problem in many large and medium-sized cities in China. China began to pay more attention to the protection and restoration of water ecological environment in 1990s, and the research on monitoring and evaluation of water ecological environment started late. Until 2015, the supervision of urban malodorous black waters has been in a blank state. In recent years, with the highly effective implementation of the „Water Ten Articles“ [4] promulgated by the State Council, the malodorous black waters have been widely concerned and actively explored by water environment experts [5]. Since May 7, 2018, the Ministry of Ecology and Environment and the Ministry of Housing and Urban-Rural Development have launched a Special Action for Environmental Protection of Malodorous Black Waters Remediation in 2018. All localities attach great importance to the problem of urban malodorous black water treatment. Because malodorous black waters are mostly small rivers, which are scattered and difficult to find, it is of great significance to carry out remote sensing identification of malodorous black waters through operational monitoring [5]. Macro-monitoring of malodorous black waters is the premise of treatment, and remote sensing technology has great advantages in macro-monitoring field [6]. Compared with the ground monitoring, the monitoring information obtained by remote sensing has the relative continuity in space and time, and the dynamic range is large, which not only helps to grasp the characteristics of the malodorous black waters from the regional level, and it is beneficial to timely and comprehensively grasp the occurrence, development, evolution and migration process of malodorous black waters, so it can save a lot of manpower, material resources and time [7].

Previous studies on malodorous black waters at home and abroad mainly focused on proposing the existence of malodorous black waters [8, 9], analyzing the formation mechanism [10, 11] and evaluation methods [12-14] of malodorous black waters, and studying sewage treatment technologies [15, 16]. However, the research on identifying and monitoring malodorous black waters by remote sensing is very rare [17]. Up to now, Jin Haixia and Pan Jian [18] have used the fused high-resolution images to retrieve various water quality parameters and monitor the malodorous black waters in Beijing. Wen Shuang et al. [19] used single-band threshold method, band difference method, band ratio method and chromaticity value to construct remote sensing identification algorithms of malodorous black waters based on GF-2 images, and compared the

classification accuracy of malodorous black waters, and concluded that the ratio algorithm had the highest identification accuracy. Hu Guoqing et al. [20] corrected the threshold value based on GF-2 image and evaluated the accuracy, and thought that the difference method was the best in single recognition algorithm. There are various types of malodorous black waters with regional and seasonal characteristics, which makes it difficult to have a unified remote sensing discrimination standard [21]. For example, the water systems in southern cities are developed, and the malodorous black waters are mainly polluted by river sludge deposition and sediment, while the water systems in northern cities are mostly short of water, and the entry of a large number of exogenous organic pollutants is the main reason for seasonal or perennial black odor in waters [17]. The research shows that the optically active substances that affect the optical properties of inland waters mainly include pure water, phytoplankton [22-24], non-algae particles [25, 26] and chromonic dispersed organic matter [27, 28]. Different waters contain different optically active substances, resulting in different absorption and reflection degrees of solar radiation energy, which makes the corresponding remote sensing reflectivity, gray scale and color scale different [29, 30].

With the development of high-score remote sensing technology, a large number of urban high-spatial resolution remote sensing data provide data support for the monitoring of urban malodorous black waters, but the research of its model method is still lacking. Thus, this study takes some areas of Zhongshan City as the research object, compares and analyzes the spectral differences between malodorous black water and normal water, and constructs a remote sensing identification model of urban malodorous black waters based on high-resolution images, in order to provide technical support for the supervision of malodorous black waters.

## Materials and Methods

### Research Area and Distribution of Sampling Points

In this study, some areas of Zhongshan City are taken as the research objects, and the suspected malodorous black waters are interpreted and identified. Zhongshan City is located in the lower reaches of the Pearl River Delta, north of Guangzhou, adjacent to Hong Kong and Macao, and across the sea from Shenzhen. It is located in the geometric center of Guangdong-Hong Kong-Macao Greater Bay Area, with a land area of 1,783.7 square kilometers. Zhongshan is one of the areas with high river network density in China. Modaomen, Hengmen and Hongqili pass through Zhongshan to the sea, with a large amount of transit water. There are more than 1,000 internal rivers and drainage channels of different scales. With the increasing population and

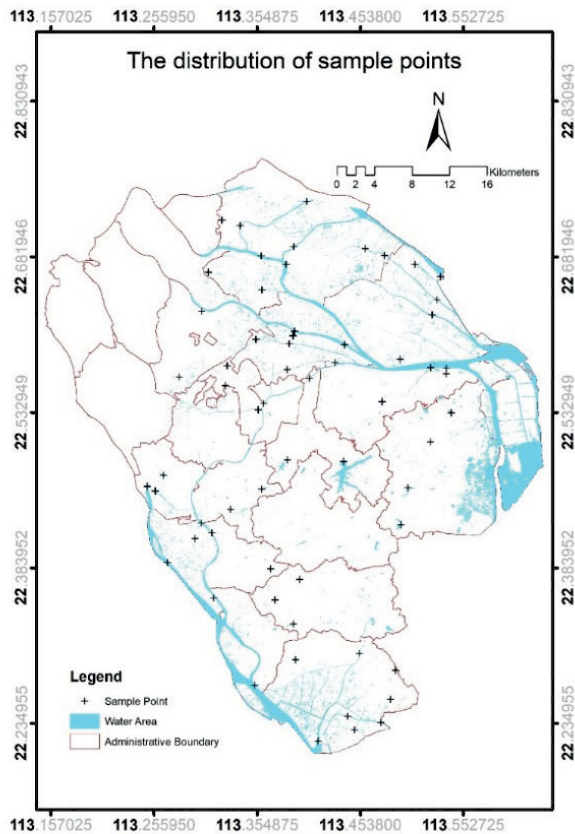


Fig. 1. Distribution of sampling points in the study area.

industrial agglomeration in recent years, the water quality of some rivers has been polluted.

A total of 62 sampling points are selected in this experiment, including malodorous black waters and normal waters. The sampling time is synchronized with the acquired remote sensing images. The distribution of specific experimental sampling points is shown in Fig. 1.

### Data and Data Preprocessing

The remote sensing images used in this study are GF -1D and GF -1C, and the image acquisition time is 11: 25 on January 1<sup>st</sup>, 2021 and 11: 25 on December 2, 2020. The spatial resolution of GF -1 C/D is 2 meters in panchromatic, better than 8 meters in multispectral, and the width of single-star imaging is more than 60 kilometers. And blue light band ranging from 0.45 to 0.52  $\mu\text{m}$ , green light band ranging from 0.52 to 0.59  $\mu\text{m}$ , red light band ranging from 0.63 to 0.69  $\mu\text{m}$  and near infrared band ranging from 0.77 to 0.89  $\mu\text{m}$ .

In this study, ENVI 5.3 was used to preprocess remote sensing images. It is necessary to install Envi app store (<https://envi.geoscene.cn/appstore/>) on ENVI 5.3. After restarting, open the App Store in Toolbox, and then install Chinese-made satellite support tools before ENVI 5.3 can load GF-1 C/D images. Then, ENVI is used for radiometric calibration, atmospheric correction, orthorectification and

image cutting. In order to prevent the result of data preprocessing from color cast, it is necessary to add the attribute of ignored value to the radiometric calibration image, and set the ignored value to 0. ENVI's own FLAASH atmospheric correction module is adopted for atmospheric correction, and the spectral reflectivity of the corresponding image points of the sample points is extracted to obtain a total of 62 groups of spectral data of the corresponding image points of the ground sampling points.

As the research scope covers a wide range, in order to keep the satellite-earth synchronous experiment as much as possible, the sampling points are selected from the water quality automatic monitoring points of Zhongshan Water Environment Comprehensive Management Platform, and the sample data are representative. According to the precise time of the remote sensing satellite flying, the water quality parameters of the sampling points are inquired, and the water sample analysis items include: dissolved oxygen, turbidity, permanganate index, ammonia nitrogen, total phosphorus and total nitrogen.

### Spectral Feature Extraction of Different Water Bodies

According to the historical monitoring data of Zhongshan Water Environment Comprehensive Management Platform, the sampling points are divided into two categories: malodorous black waters and normal waters. The pixels of malodorous black waters and normal waters are found on GF-1D of January 1<sup>st</sup>, 2021. Excluding the influence of surrounding mixed pixels, all the pixels are pure pixels, and the average operation is completed with the adjacent pure pixels. The spectral curves of typical malodorous black waters and normal waters are obtained by statistical analysis of remote sensing reflectance of these pixels in Envi 5.3 software.

### Identification Model of Malodorous Black Waters

At present, NDBWI [31] and BOI [32] are commonly used in the research of remote sensing information extraction of malodorous black waters. Among them, NDBWI index reflects the difference between malodorous black waters and normal waters by using the characteristic that the spectral curve of malodorous black waters changes gently in the red and green bands, and using the ratio of difference and sum. The specific formula is as follows [33]:

$$NDBWI = [Rrs(G) - Rrs(R)]/[Rrs(G) + Rrs(R)] \quad (1)$$

In the formula, Rrs(G) is the remote sensing reflectivity of green light band and B2 band for GF-1 satellite; Rrs(R) is the remote sensing reflectivity of red light band and B3 band for GF-1 satellite.

BOI (Black and Odorous Water Index) is a normalized ratio model, which is constructed by using the difference of spectral characteristics between green and red light bands, in which the remote sensing reflectance of normal water decays rapidly while the change of malodorous black waters is not obvious [34]. Specific formula:

$$BOI = [Rrs(G) - Rrs(R)]/[Rrs(B) + Rrs(G) + Rrs(R)] \quad (2)$$

In the formula, Rrs(B) is the remote sensing reflectivity of blue light band, and is B1 band for GF-1 satellite; Rrs(G) is the remote sensing reflectivity of green light band, and is B2 band for GF-1 satellite; Rrs(R) is the remote sensing reflectivity of red light band, and is B3 band for GF-1 satellite; T is the threshold of malodorous black waters.

According to the reflectance spectrum characteristics of malodorous black waters and normal waters, this study tries to identify the spatial distribution of malodorous black waters by strengthening the difference information between malodorous black waters and normal waters. This study attempts to model the band combination in the process of searching for the best band with the following two ideas: 1. Find the band with strong reflectivity and the band with weak reflectivity, and calculate the difference between them to enlarge the gap between the two types of waters; 2. Referring to the normalized ratio model, the difference between the two types of waters is enlarged by the method of composite band ratio, in order to find the best band combination mode. The band combination model is as follows:

$$HCI1 = B4 - B1 \quad (3)$$

$$HCI2 = B3 + B4 - B1 \quad (4)$$

$$HCI3 = B3 + B4 - B2 \quad (5)$$

$$HCI4 = (B4 - B1)/(B1 + B4) \quad (6)$$

$$HCI5 = (B3 + B4 - B1)/(B1 + B3 + B4) \quad (7)$$

$$HCI6 = (B3 + B4 - B2)/(B2 + B3 + B4) \quad (8)$$

Where, for GF-1 satellite, B1 represents Rrs(B), which is the remote sensing reflectivity of blue band; B2 represents Rrs(G), which is the remote sensing reflectivity of green band; B3 represents Rrs(R), which is the remote sensing reflectivity of red band; B4 represents Nir(R), which is the remote sensing reflectivity of near-infrared band.

After establishing the discrimination model of malodorous black waters, malodorous black waters can be distinguished from normal waters by looking for a reasonable threshold. The discrimination formula of pixel identification is:

$$HCI > k \quad (9)$$

Where, k represents the threshold for distinguishing malodorous black waters and normal waters.

### Evaluation of Identification Accuracy

In Arcgis, the sampling points are superimposed with the classification results to check whether the sampling points fall into the corresponding water body types, so as to test the classification accuracy of the model [35]. In order to judge the classification accuracy of the identification indexes of malodorous black waters more scientifically and reasonably, this study introduces the kappa coefficient method in the confusion matrix [36]. Kappa coefficient can determine whether the difference between the actual coincidence rate and the random coincidence rate is significant. Kappa coefficient is obtained by multiplying the total number of pixels in all real land surface classifications by the sum of diagonal lines of confusion matrix, subtracting the product of the total number of real land surface pixels and the total number of classified pixels in that class, and then dividing by the square of the total number of pixels and subtracting the product of the total number of real land surface pixels and the total number of classified pixels in that class. The specific formula is as follows [37]:

$$k = \frac{p_o - p_e}{1 - p_e} \quad (10)$$

Where,  $p_o$  is the sum of the number of correctly classified samples in each category divided by the total number of samples, which is the overall classification accuracy. Assuming that the real sample number of each class is  $a_1, a_2, \dots, a_C$ , and the predicted sample number of each class is  $b_1, b_2, \dots, b_C$ , and the total sample number is  $n$ , there are:

$$p_e = \frac{a_1 \times b_1 + a_2 \times b_2 + \dots + a_C \times b_C}{n \times n} \quad (11)$$

The calculation result of Kappa is between -1 and 1, but Kappa coefficients usually vary between 0 and 1. It can be divided into five groups to represent different levels of consistency: slight consistency (0.0-0.20), fair consistency (0.21-0.40), moderate consistency (0.41-0.60), substantial consistency (0.61-0.80), and almost perfect consistency (0.81-1).

## Results and Discussion

### Analysis of Spectral Characteristics of Water Reflectivity

By comparing the spectral characteristics of malodorous black waters and normal waters of

Zhongshan City, it is found that malodorous black waters had a significant change in the green band of 0.57  $\mu\text{m}$  and the red band of 0.68 $\mu\text{m}$ , especially the red band of 0.68  $\mu\text{m}$  is more significant (Fig. 2), and normal waters had a significant peak in the green band of 0.57  $\mu\text{m}$  (Fig. 3). In the near red band and red band, the spectral characteristics of malodorous black waters are obviously higher than that of normal waters. In the green band, the spectral characteristics of normal waters appear a fluorescence peak at 0.57  $\mu\text{m}$ , which reflects the spectral characteristics difference between malodorous black waters and normal waters. In the blue band, the spectral characteristics of normal waters are slightly higher than that of malodorous black waters. In the near infrared band, the spectral characteristics of malodorous black waters are much higher than that of normal waters. Therefore, discrimination model on malodorous black waters can be established according to the above rules. The spectral characteristics differences between malodorous black waters and normal waters can be used as an important basis for remote sensing recognition, and provide a basis for the selection of the best band or band combination of remote sensing quantitative inversion model.

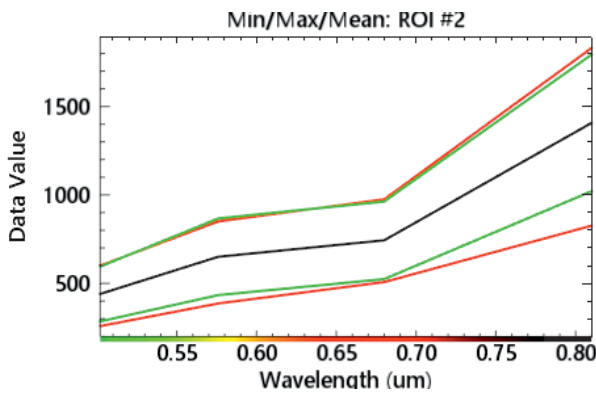


Fig. 2. Spectral curve of malodorous black waters.

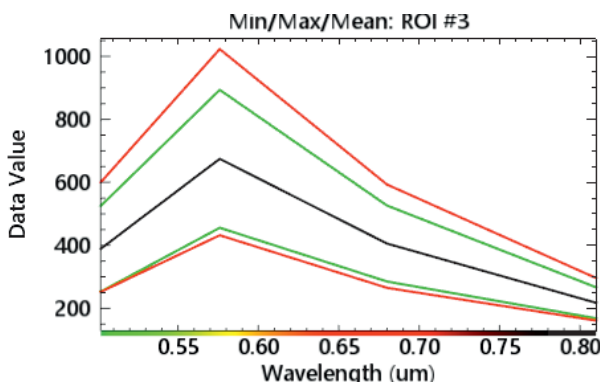


Fig. 3. Spectral curve of normal waters.

### Threshold Division of Malodorous Black Water Identification

Using NDWI (Normalized Water Body Index) to extract the water body in the study area, and then importing it into Arcgis to process the conversion layer for export. Then, malodorous black waters discrimination models are used to identify the normal waters and malodorous black waters. The calculation results of each model are shown in Fig. 4.

In order to obtain an appropriate threshold range, according to the water quality monitoring data of Zhongshan Water Environment Comprehensive Management Platform, the samples of malodorous black waters and normal waters were selected, and the indexes were calculated to draw box diagrams (Fig. 5).

According to the analysis of the above box diagram, it is found that the numerical distribution of the three index models of NDBWI, BOI and HCI5 can be distinguished between the malodorous black waters and normal waters. The threshold division of the three index models are shown in the red line and the red letter on the box diagram: NDBWI = 0.09, BOI = 0.06, HCI5 = 0.4, the specific division effect needs to be further verified. However, the overlap ratio of other index models is significant, so the default value of the natural break point method is adopted as the threshold, which are: HCI1 = -0.010, HCI2 = 0.088, HCI3 = 0.044, HCI4 = -0.127, HCI6 = 0.141. The model threshold selected by the model is applied to obtain the classification map of malodorous black waters and normal waters on the basis of Fig. 4 (Fig. 6), where the red part is the defined range of malodorous black waters, and the green part is the defined range of normal waters.

### Accuracy Evaluation of Malodorous Black Water Identification

Fig. 7 is the water quality classification map of sampling points according to the water quality monitoring data of Zhongshan Water Environment Comprehensive Management Platform on January 1<sup>st</sup>, 2021, which is used to test the identification accuracy of each model. The test and analysis results are shown in Table 1. The results show that both NDBWI and BOI index model have 16 malodorous black water points correctly classified, but BOI index model has a higher identification accuracy than NDBWI for normal water.

Among the six HCI index models proposed in this study, HCI2 and HCI5 achieved 100% accuracy in normal waters identification, but HCI2 was not correct in malodorous black waters identification, while HCI5 correctly identified 15 malodorous black water points, so HCI5 also had a good performance. In addition, HCI1 and HCI4 performed well in the identification of malodorous black waters, but the identification of normal waters was poor. For example, 18 normal water points were incorrectly identified in HCI1, and

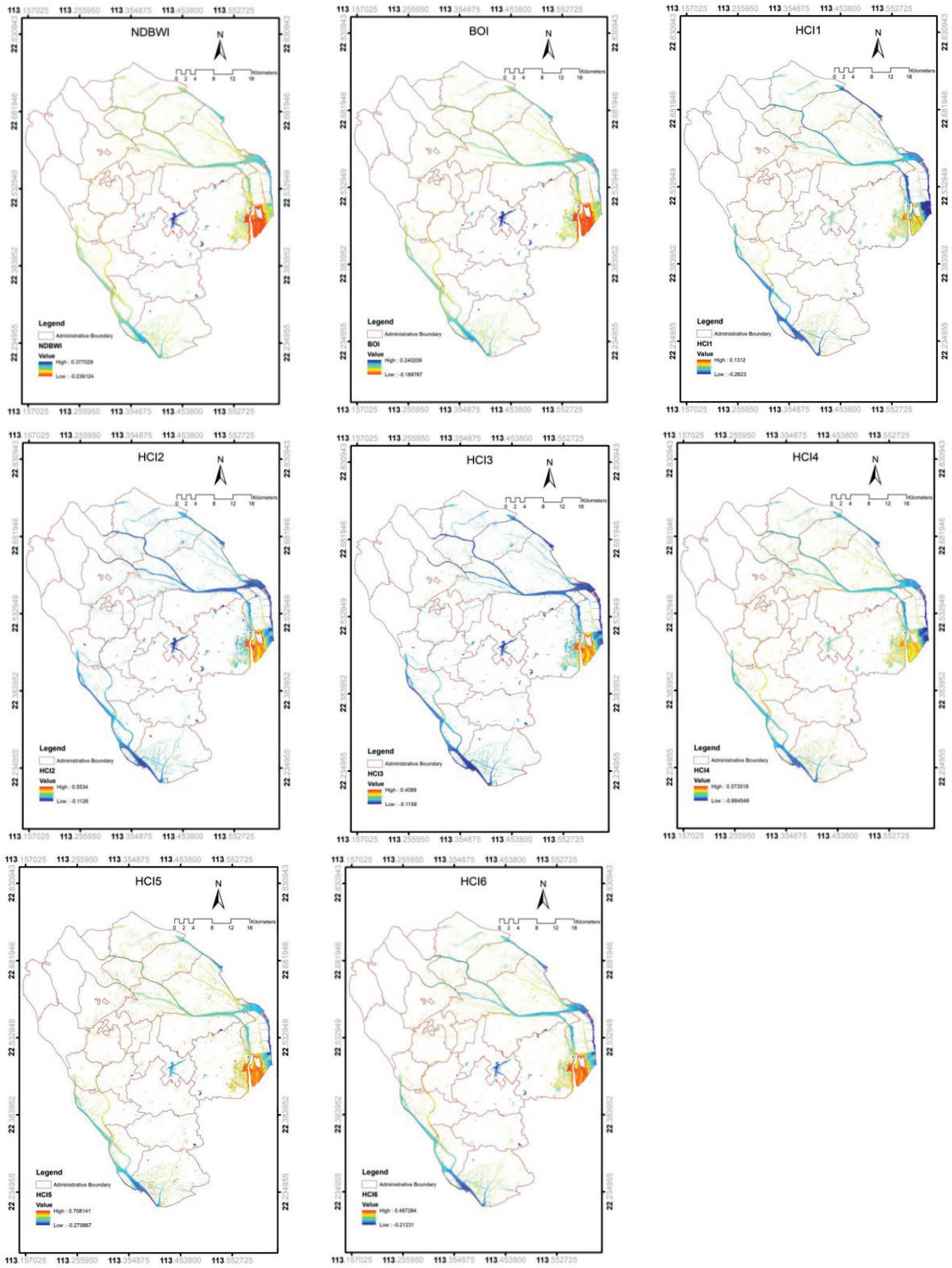


Fig. 4. Results of each model within the waters area.

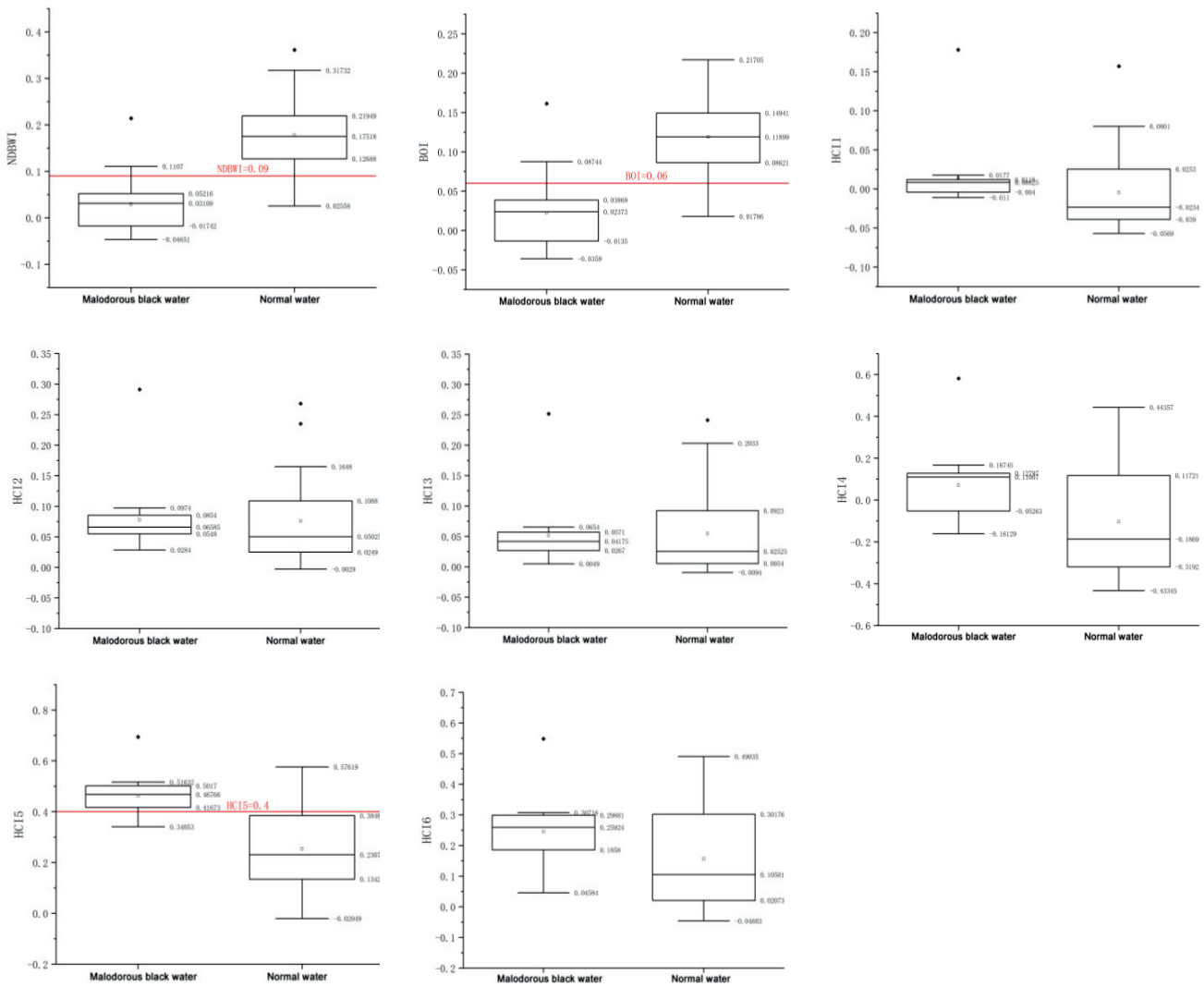


Fig. 5. Box diagrams of each model.

11 normal water points were incorrectly identified in HCI4. Considering the identification of malodorous black waters and normal waters, HCI1 and HCI4 did not perform as well as BOI and HCI5.

Furthermore, the Kappa coefficient was used to determine whether there was a significant difference between the actual consensus rate and the random consensus rate. The actual water samples identification results and the water samples identification results predicted by the model were tabled, and the Kappa coefficient analysis was completed by SPSS. The results are shown in Table 2. It shows that the highest Kappa coefficient is HCI5 (0.876) and BOI (0.843), followed by NDBWI (0.739) and HCI4 (0.608). Other models have poor identification accuracy.

#### Universality Analysis of Malodorous Black Water Identification Model

According to the above identification accuracy evaluation, BOI and HCI5 models can accurately distinguish malodorous black waters from normal

waters. In order to study the effectiveness of the above-mentioned model threshold in a certain range for high-scoring images and avoid contingency, the experiment further used the GF-1C remote sensing images on December 2<sup>nd</sup>, 2020 and water quality monitoring data of Zhongshan Water Environment Comprehensive Management Platform on December 2<sup>nd</sup>, 2020 to conduct the universality study of the model threshold.

The above method steps were repeated to obtain the water identification results using BOI and HCI5 models on December 2<sup>nd</sup>, 2020 (Fig. 8), and the accuracy evaluation and the identification results were compared (Table 3 and Table 4). From the perspective of the universality of the threshold, BOI used the 123 band with a threshold of 0.06, and HCI5 used the 134 band with a threshold of 0.4. When applied to remote sensing images of other time phases, malodorous black waters can still be distinguished from normal waters. Therefore, BOI and HCI5 models have high accuracy evaluation and universality for malodorous black waters.

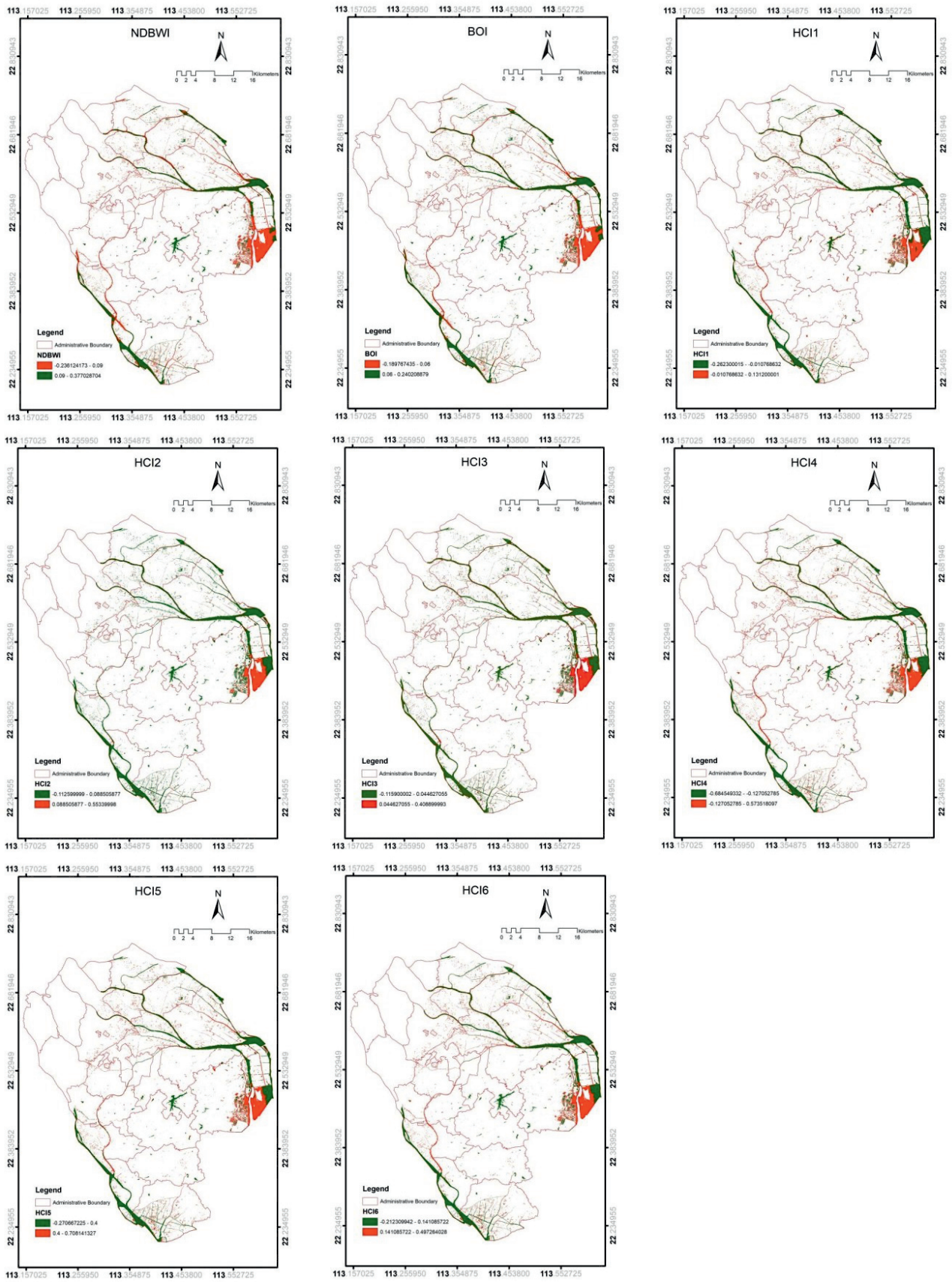


Fig. 6. Identification results of malodorous black waters with different index models.

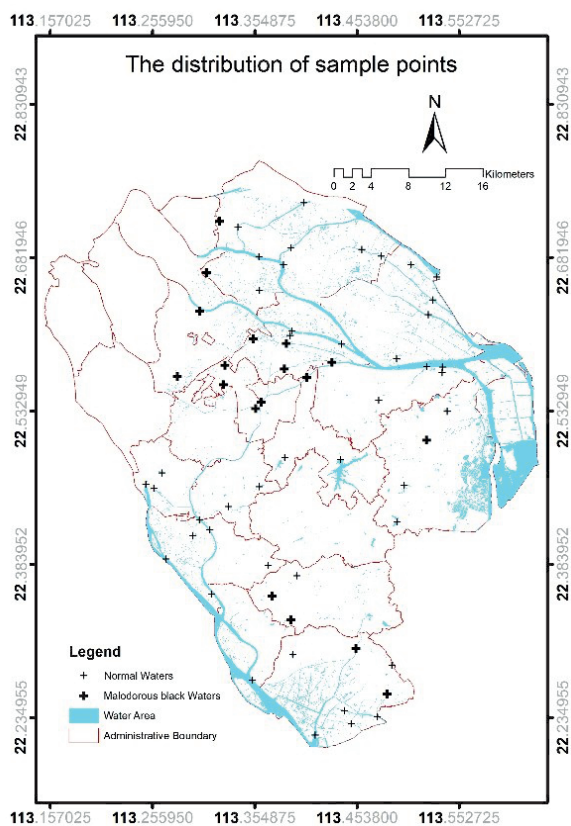


Fig. 7. Water quality sampling points on January 1<sup>st</sup>, 2021.

Table 2. Kappa coefficient analysis of different models.

Model	Threshold	Kappa coefficient
NDBWI	0.09	0.739
BOI	0.06	0.843
HCI1	-0.010	0.442
HCI2	0.088	Invalid data
HCI3	0.044	0.475
HCI4	-0.127	0.608
HCI5	0.4	0.876
HCI6	0.141	0.529

### Discussion

The selection of experimental sampling points is the key of this study. The sampling points should have a certain distribution breadth, and they should be representative and typical. As many sample points as possible will help to improve the accuracy of the models. Since the water quality data at sampling points should be synchronized with remote sensing spectral data, the on-site water quality sampling will consume a lot of manpower and material resources, and it is difficult to ensure the synchronization of time. In view of this consideration, this experiment is optimized on the basis of monitoring points of Zhongshan Water Environment Comprehensive Management Platform.

Table 1. Threshold and water identification of different models.

Model	Type	Threshold	Correct identification
NDBWI	Malodorous black waters	0.09	16/18
	Normal waters		39/44
BOI	Malodorous black waters	0.06	16/18
	Normal waters		42/44
HCI1	Malodorous black waters	-0.010	17/18
	Normal waters		27/44
HCI2	Malodorous black waters	0.088	0/18
	Normal water		44/44
HCI3	Malodorous black waters	0.044	7/18
	Normal waters		32/44
HCI4	Malodorous black waters	-0.127	18/18
	Normal waters		33/44
HCI5	Malodorous black waters	0.4	15/18
	Normal waters		44/44
HCI6	Malodorous black waters	0.141	16/18
	Normal waters		32/44

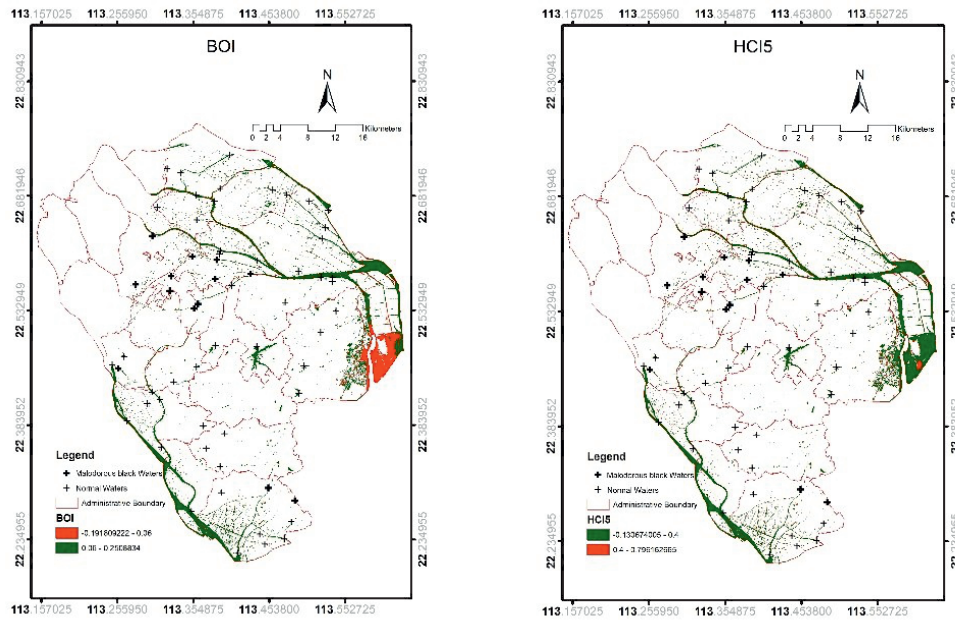


Fig. 8. Identification results of BOI and HCI5 models for malodorous black waters.

Table 3. Water identification of different models.

Model	Type	Threshold	Correct identification
BOI	Malodorous black waters	0.06	10/12
	Normal waters		48/50
HCI5	Malodorous black waters	0.4	8/12
	Normal waters		49/50

Although the spatial resolution of panchromatic band of GF-1 B/C/D can reach 2 meters, we attempted to perform image fusion of 8 meters in multispectral and 2 meters in panchromatic, and then extracted water spectral feature. Compared with the spectral features of water extracted by simply using multi-spectral bands, there is a large gap in the sample data at the location of fine rivers, so the spatial resolution of remote sensing images in this experiment is still 8 meters. Due to the limitation of spatial resolution, the sampling point must be located in a river water area of no less than 8 meters. Moreover, considering that the pixels selected in the image are required to be pure pixels, the influence of surrounding mixed pixels should be excluded, so the actual selected sampling points will be located in a wider water area. In fact, malodorous

black waters are more likely to appear at the scale of small rivers. Therefore, the selection of GF-1 B/C/D in this experiment has some shortcomings, that is, the selection of water sampling points scale is limited, resulting in a small number of malodorous black waters in water sampling points. If GF-2 or other higher resolution images are used, the problem of sampling point selection scale can be solved. However, since the width is not as wide as GF-1 and GF-1 B/C/D, image piecing is often needed for large research areas, and the consistency of image time is difficult to ensure, which has a great impact on the experiment. In addition, it is easy to appear seams in image piecing, and it is necessary to carry out color adjustment, matching and fusion, and other operations, which will cause errors in spectral feature extraction.

Table 4. Kappa coefficient analysis.

Model	Threshold	Kappa coefficient
BOI	0.06	0.793
HCI5	0.4	0.715

The classification errors of different malodorous black waters identification models are mainly due to the overlap of spectra. From the box diagrams of each model in Fig. 5, it is not difficult to see that HCI1, HCI2, HCI3, HCI4 and HCI6 all have large overlap, so it is difficult to judge the threshold of these models. The natural breakpoint method is used to divide the threshold, which is uncertain due to the different

research objects. Therefore, these identification models are not recommended.

Comparing the identification accuracy of different models, the ratio algorithm (NDBWI, BOI, HCl4, HCl5 and HCl6) is significantly higher than the difference algorithm (HCl1, HCl2, HCl3). On the basis of the general normalized ratio model, the method of compound band ratio is adopted, that is, to add one or more band combinations to the original single normalized model, so as to constitute the identification model of malodorous black waters. It is feasible to find the best band combination to establish the identification model of malodorous black waters.

Zhongshan is located in the south of the Tropic of Cancer and belongs to the south subtropical monsoon climate, with distinct dry and wet conditions and the same period of hot and rainy, and the summer is long and rainy. Therefore, remote sensing images in this region in summer are often covered with extreme cloud cover, which cannot be applied to this study. It will be more convincing to use remote sensing images of different seasons to analyze the universality of the identification model. In the future, UAV remote sensing images can be used to supplement the shortcomings of the existing remote sensing images in time series.

### Conclusion

The spectral characteristics of malodorous black waters were different from those of normal waters. It was found that the malodorous black waters had a significant change in the green band of 0.57  $\mu\text{m}$  and the red band of 0.68  $\mu\text{m}$ , especially the red band of 0.68  $\mu\text{m}$ , and the normal waters had a significant peak in the green band of 0.57  $\mu\text{m}$ . The spectral differences between malodorous black waters and normal waters can be used as an important basis for remote sensing identification.

Based on the differences in spectral characteristics between malodorous black waters and normal waters, the identification models of HCl1-6, which are established respectively based on multi-spectral bands 1, 2, 3, and 4 of GF-1D, and compared with the NDBWI and BOI index models. Selecting different water quality samples to draw the box diagrams of each index model as an important basis for defining the threshold, NDBWI threshold is 0.09, the BOI threshold is 0.06 and the HCl5 threshold is 0.4.

Using the synchronous monitoring results of surface water quality to evaluate the identification accuracy of malodorous black waters, and the Kappa coefficient was used to determine whether there was a significant difference between the actual consensus rate and the random consensus rate. By comparison, the recognition accuracy of the ratio algorithm is significantly higher than the difference algorithm, that is, add one or more band combinations to the original single normalized

model, so as to constitute the identification model of malodorous black water. It is feasible to find the best band combination to establish the identification model of malodorous black water. The Kappa coefficient is the highest in HCl5 (0.876) and BOI (0.843), followed by NDBWI (0.739) and HCl4 (0.608). Other models have poor identification accuracy.

In order to study the effectiveness of the BOI and HCl5 models threshold on high-resolution images within a certain range and avoid contingency, this experiment carried out a universality study of the model threshold. After verification, BOI used the 123 band with a threshold of 0.06, and HCl5 used the 134 band with a threshold of 0.4. When BOI and HCl5 index models are applied to other remote sensing image, they can still distinguish black and malodorous black waters from normal waters. Accordingly, this study suggests that BOI and HCl5 should be used as index models for remote sensing identification of malodorous black water in Zhongshan City.

### Acknowledgments

The authors would like to thank Zhongshan Water Affairs Bureau and Zhongshan Water Environmental Treatment Co., Ltd. for providing the data support in the study. Funding from major public welfare projects in Zhongshan is gratefully acknowledged.

### Conflict of Interest

The authors declare no conflict of interest.

### References

1. Ministry of Housing and Urban-Rural Development. Guidelines for remediation of urban black and odorous water bodies. Beijing, **2015**.
2. TANG J., PANG W.H., LIN C.Y., HUANG, J., JIE, H., LIAO Y. Cause analysis and comprehensive treatment technology of black and odorous water bodies in China. *Applied Chemical Engineering*. **49** (2), 483, **2020**.
3. WANG X., WANG Y.G., SUN C.H., TAO P. Research progress of formation mechanism and evaluation method of urban black and odorous water body. *Journal of Applied Ecology*. **27** (4), 1331, **2016**.
4. State Council of the People's Republic of China. Action Plan for Water Pollution Prevention and Control. Beijing, **2015**.
5. CAO J.N. Research on remote sensing interpretation algorithm of black and odorous water body based on fuzzy decision tree. *North china institute of aerospace engineering*. **2021**.
6. CHEN S., ZHAO W.Y., LIAO Z.P. Research progress of remote sensing identification of black and odorous water bodies. *Remote Sensing of Land and Resources*. **33** (1), 20, **2021**.
7. LI L. Study on water quality grade discrimination of urban small and medium-sized rivers based on UAV

- hyperspectral remote sensing. University of Chinese Academy of Sciences (Shanghai Institute of Technical Physics, Chinese Academy of Sciences). **2021**.
8. LIAO W.L., HUANG J.S., DING J.G., LIU M., CHEN T.T., TONG Q.B., YAO Y., LU S.H. Research status of black and odorous water pollution and remediation technology in China. *Journal of yangtze river scientific research institute*. **34** (11), 153, **2017**.
  9. LI B., BAI Y.W., LIU D.N., WANG F., YUAN P., LIU R.X. Distribution, existing problems and countermeasures of black and odorous water bodies in built-up areas of prefecture-level cities and above. *Journal of Environmental Engineering*. **13** (3), 511, **2019**.
  10. CUI W., ZHANG Y., HUANG M. Activities of urease and phosphatase in integrated vertical flow constructed wetland and purification effect of black and malodorous river. *Agricultural Science & Technology-Hunan*. **12** (8), 1186, **2011**.
  11. CHEN J., XIE P., MA Z., NIU Y., TAO M., DENG X., WANG Q. A systematic study on spatial and seasonal patterns of eight taste and odor compounds with relation to various biotic and abiotic parameters in Gonghu Bay of Lake Taihu, China. *Science of The Total Environment*. **409** (2), 314, **2010**.
  12. SUGIURA N., UTSUMI M., WEI B., IWAMI N., OKANO K., KAWAUCHI Y., MAEKAWA T. Assessment for the complicated occurrence of nuisance odours from phytoplankton and environmental factors in a eutrophic lake. *Lakes & Reservoirs: Research & Management*. **9** (3-4), 195, **2004**.
  13. GU QIANG., DING LEI. Comparison of evaluation methods of black and odorous water bodies in urban built-up areas. *Water Resources Protection*. **33** (4), 70, **2017**.
  14. LU B.Y., BAI H.Q. Evaluation index and evaluation method of black and odorous water body. *Chemical Engineer*. **35** (10), 56, **2021**.
  15. NI S., HUANG C., HUANG Y., LI Z., XU J., HUANG F., JIA J. Demonstration research project of a new three-stage bio-oxidation pond for purifying black smelly water bodies. *Journal of Water Process Engineering*. **47** (6), 102695, **2022**.
  16. SHI F., LIU Z., LI J., GAO H., QIN S., GUO J. Alterations in microbial community during the remediation of a black-odorous stream by acclimated composite microorganisms. *Journal of Environmental Sciences*. **118** (8), 181, **2022**.
  17. SHEN QIAN., ZHU LI., CAO H.Y. Research progress of remote sensing monitoring and screening of urban black and odorous water bodies. *Journal of Applied Ecology*. **28** (10), 3433, **2017**.
  18. JIN H.X., PAN J. Remote sensing monitoring of urban black and odorous water body based on the fusion data of Gaofen-2 satellite. *Science and Technology Management of Land and Resources*, **34** (4), 107, **2017**.
  19. WEN S., WANG Q., LI Y.M., ZHU L., LU H., LEI S.H., DING X.L., MIAO S. Remote sensing identification of urban black and odorous water bodies based on high-resolution images: taking Nanjing as an example. *Environmental Science*, **39** (1), 57, **2018**.
  20. HU G.Q., CHEN D.H., LIU C.F., XIE Y.M., LIU S.S., LI, H. Dynamic monitoring of urban black and odorous water body based on Gaofen-2. *Remote Sensing of Land and Resources*. **33** (1), 30, **2021**.
  21. WU A. *River Health Assessment: Theory, Method and Practice*. East China Normal University. **2008**.
  22. SONG T., ZHOU W.L., LIU J.Z., GONG S.Q., SHI J.Z., WU W. Evaluation of chlorophyll a concentration distribution in Taihu Lake by hyperspectral inversion model. *Journal of Environmental Science*. **37** (3), 888, **2017**.
  23. HU M., ZHANG Y., MA R., XUE K., CAO Z., CHU Q., JING Y. Optimized remote sensing estimation of the lake algal biomass by considering the vertically heterogeneous chlorophyll distribution: Study case in Lake Chaohu of China. *Science of The Total Environment*. **771** (6), 144811, **2021**.
  24. HE J., CHEN Y., WU J., STOW D.A., CHRISTAKOS G. Space-time chlorophyll-a retrieval in optically complex waters that accounts for remote sensing and modeling uncertainties and improves remote estimation accuracy. *Water Research*. **171** (3), 115403, **2020**.
  25. LU X.M., SU H. Remote sensing inversion of suspended matter concentration in Fujian coastal waters based on OLCI data. *Journal of Environmental Science*. **40** (8), 2819, **2020**.
  26. PETERSON K.T., SAGAN V., SIDDIKE P., COX A.L., MARTINEZ M. Suspended Sediment Concentration Estimation from Landsat Imagery along the Lower Missouri and Middle Mississippi Rivers Using an Extreme Learning Machine. *Remote Sensing*. **10** (10), 1503, **2018**.
  27. NEZLIN N.P., BEEGAN C., FEIT A., GULLY J.R., LATKER A., MCLAUGHLIN K., MENGEL M.J., ROBERTSON G.L., STEELE A., WEISBERG S.B. Colored Dissolved Organic Matter (CDOM) as a tracer of effluent plumes in the coastal ocean. *Regional Studies in Marine Science*. **35** (3), 101163, **2020**.
  28. BREZONIK P.L., OLMANSON L.G., FINLAY J.C. BAUER M.E. Factors affecting the measurement of CDOM by remote sensing of optically complex inland waters. *Remote Sensing of Environment*. **157** (2), 199, **2015**.
  29. ROSTOM N.G., SHALABY A.A., ISSA Y.M., AFIFI A.A. Evaluation of Mariut Lake water quality using Hyperspectral Remote Sensing and laboratory works. *The Egyptian Journal of Remote Sensing and Space Science*. **20** (4), S39, **2017**.
  30. TIIT K., BIRGOT P., CHARLES V., MARTIN L., TUULI S., KAIRE T., GEMA C. Remote Sensing of Black Lakes and Using 810 nm Reflectance Peak for Retrieving Water Quality Parameters of Optically Complex Waters. *Remote Sensing*, **8** (6), 497, **2016**.
  31. JIANG Y.W., ZHOU N., ZHOU Y.Y., HUANG R.J., ZHONG Z. Study on remote sensing dynamic monitoring method of urban black and odorous water body. *Bulletin of Surveying and Mapping*. (S1), 98, **2019**.
  32. YAO Y., SHEN Q., ZHU L., GAO H.J., CAO H.Y., HAN H., SUN J.G., LI J.S. The remote sensing identification of black and odorous water bodies in Shenyang of Gaofen No. 2. *Journal of Remote Sensing*. **23** (02), 230, **2019**.
  33. HAN W.C., ZHANG X.Y., CHEN J.X., WANG T.G., SHANG Y.S., DING Y.J. Remote sensing monitoring of urban black and odorous water based on Gaofen-2 image. *Environmental Ecology*. **3** (01), 63, **2021**.
  34. YAO Y. Research on identification model of urban black and odorous water body based on GF multispectral images. *Lanzhou Jiaotong University*. **2018**.
  35. JI G. Research and application of black and odorous water body identification method based on remote sensing. *Lanzhou Jiaotong University*. **2017**.

- 
36. GUO Y.B., GUO W., QIN Y.C., HE Q., ZHANG X.J., WU C. Consistency test based on Kappa coefficient and its software implementation. *China Health Statistics*. **33** (01), 169, **2016**.
37. WANG X.R., PAN P.P., WANG X.X., WANG X.M. Simulation of land use landscape pattern in Hebei Province based on GeoSOS-FLUS model. *Jiangsu journal of agricultural sciences*. 37 (03), 667, **2021**.